

Isotope effect on the anomalies of water: a corresponding states analysis

Frédéric Caupin,^{a)} Pierre Ragueneau, and Bruno Issenmann^{b)}

Institut Lumière Matière, Université Claude Bernard Lyon 1, CNRS, Institut Universitaire de France, F-69622, Villeurbanne, France

(Dated: 16 May 2024)

Light and heavy water show similar anomalies in thermodynamic and dynamic properties, with a consistent trend of anomalies occurring at higher temperature in heavy water. Viscosity also increases faster upon cooling in heavy water, causing a giant isotope effect, with a viscosity ratio near 2.4 at 244 K. While a simple temperature shift apparently helps in collapsing experimental data for both isotopes, it lacks a clear justification, changes value with the property considered, and requires additional *ad hoc* scaling factors. Here we use a corresponding states analysis based on the possible existence of a liquid-liquid critical point in supercooled water. This provides a coherent framework which leads to the collapse of thermodynamic data. The ratio between dynamic properties of the isotopes is strongly reduced. In particular, the decoupling between viscosity η and self-diffusion D , measured as a function of temperature T by the Stokes-Einstein ratio $D\eta/T$, is found to collapse after applying the corresponding states analysis. Our results are consistent with simulations and suggest that the various isotope effects mirror the one on the liquid-liquid transition.

INTRODUCTION

At ambient conditions, water (H_2O) and its fully deuterated isotope, deuterium oxide (D_2O), have almost identical molar volume or surface tension, but their shear viscosities differ by nearly 25%. Isotopic content matters for higher living organism, high doses of heavy water being lethal, because of slowing down of chemical reaction kinetics¹. Heavy water exhibits the same anomalies that are found in light water²⁻⁴, e.g. density maximum, isothermal compressibility and isobaric heat capacity minima near ambient temperature, or non-monotonic pressure dependence of viscosity and diffusivity at low temperature. In both isotopes, these anomalies get more pronounced when the liquid enters the supercooled region, below the ice-liquid equilibrium temperature. Several theories have been put forward to explain these anomalies, including the existence of a metastable phase transition between two distinct supercooled liquids⁵. Experiments supporting this possibility have been reported for H_2O : a first-order like transition between two glassy phases of water, differing in structure and density⁶, and a discontinuity in decompression-induced melting lines of high-pressure ices⁷. The two amorphous ices⁸ and the melting line discontinuity⁹ are also found in D_2O .

One of the strongest contrast between H_2O and D_2O is observed for their dynamic properties. Figure 1 shows the ratios $\eta_r = \eta_{\text{D}}/\eta_{\text{H}}$, $D_r = D_{\text{H}}/D_{\text{D}}$, and $\tau_{\theta,r} = \tau_{\theta,\text{D}}/\tau_{\theta,\text{H}}$, where η is the shear viscosity, D the self-diffusion coefficient, and τ_{θ} the rotational correlation time, respectively, and subscripts H and D refer to the light and heavy isotope, respectively. All experimental data used in this work are presented in Tables I and II for H_2O and D_2O , respectively. Our recent viscosity data^{10,11} allow us to plot η_r to lower temperature than before. It reaches a massive 2.38 at 243.7 K, which, to our knowledge, is only

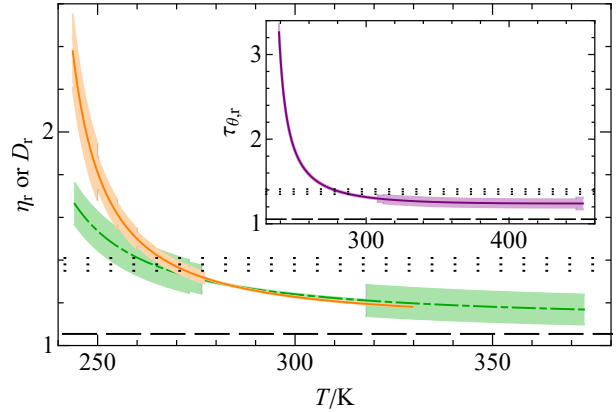


FIG. 1. Isotope effect for viscosity ($\eta_r = \eta_{\text{D}}/\eta_{\text{H}}$, solid orange curve) and self-diffusion ($D_r = D_{\text{H}}/D_{\text{D}}$, dash-dotted green curve) for water. The values of $\sqrt{M_r}$ and $\sqrt{I_r}$ are shown with horizontal dashed and dotted lines, respectively. The inset displays the isotope effect for the rotational correlation time ($\tau_r = \tau_{\theta,\text{D}}/\tau_{\theta,\text{H}}$, purple curve). The colored areas denote the $1 - \sigma$ uncertainties.

exceeded by quantum liquids: helium 4, which becomes superfluid at higher temperature than helium 3; and the hydrogen isotopes, H_2 and D_2 , for which $\eta_r \simeq 3$ ¹². $\tau_{\theta,r}$ reaches an even higher value, 3.26 at 239 K.

To reconcile density and viscosity data for light and heavy water, Robinson and collaborators introduced the thermal offset hypothesis¹³⁻¹⁵. We first present this approach and its limitations. Then, we attempt another analysis, based on the idea of corresponding states¹⁶⁻¹⁹. Assuming the existence of a liquid-liquid critical point terminating a metastable liquid-liquid transition in supercooled water³, we show how a simple rescaling of temperature and pressure by the critical values leads to a striking collapse of thermodynamic and dynamic data for the two isotopes. We finally discuss the connection of our corresponding states analysis with the thermal off-

^{a)} frederic.caupin@univ-lyon1.fr

^{b)} bruno.issenmann@univ-lyon1.fr

TABLE I. Properties of light water used in this study. The last column indicates the type of fitting function used in the calculations for comparison with heavy water data.

Ref.	P (MPa)	T range (K)	Fitting function
Molar volume V_{mol}			
20	0.1	239.74 – 267.92	8-th order
21 ^a	0.1	273.15 – 313.15	polynomial
Isothermal compressibility κ_T			
22	10	250.35 – 297.95	4-th order polynomial
22	50	248.15 – 298.15	4-th order polynomial
22	100	240.95 – 298.05	4-th order polynomial
Isobaric heat capacity C_P			
23	0.1	236.01 – 290	6-th order polynomial
Viscosity η			
11 ^b	0.1	239.15 – 491.95	Speedy-Angell law ^d
Self-diffusion coefficient D			
10 ^c	0.1	237.8 – 498.2	Speedy-Angell law ^d
Rotational correlation time τ_θ			
10 ^c	0.1	236.2 – 451.6	Speedy-Angell law ^d

^a We used this formulation to compute V_{mol} values every 5 K.

^b This reference compiles data from a series of sources^{10,24–30}.

^c This reference compiles data from a series of sources for D ^{31–34} and for τ_θ ^{35,36}.

^d $X(T) = X_0(T/T_s - 1)^{-\gamma}$, with parameters X_0 , T_s , and γ given in Ref. 11 for $X = \eta$, and in Ref. 10 for $X = D$ and τ_θ . The fits are valid up to 348.15 K, 498.2 K, and 451.63 K for η , D , and τ_θ , respectively.

TABLE II. Properties of heavy water used in this study.

Ref.	P (MPa)	T range (K)
Molar volume V_{mol}		
2 ^a	0.1	244.1 – 313.14
37 ^b	0.1	258.15 – 298.15
Isothermal compressibility κ_T		
22	10	253.36 – 297.8
22	50	248.9 – 298
22	100	244.2 – 297.9
Isobaric heat capacity C_P		
23	0.1	236.01 – 290
Viscosity η		
11 ^c	0.1	243.7 – 493.05
Self-diffusion coefficient D		
11 ^c	0.1	244.2 – 623
Rotational correlation time τ_θ		
11 ^c	0.1	239.0 – 473.15

^a This reference compiles data from a series of sources^{38–43}.

^b Values from Table V of Ref. 37.

^c This reference compiles data from a series of sources for η ^{29,44–49}, D ^{31,50–55}, and τ_θ ^{36,54,56–60}.

set hypothesis and with other works on the liquid-liquid transition in water.

THE THERMAL OFFSET HYPOTHESIS

The thermal offset concept. In a series of works^{13–15}, Robinson and collaborators proposed that several properties of D₂O can be deduced from those of H₂O by a

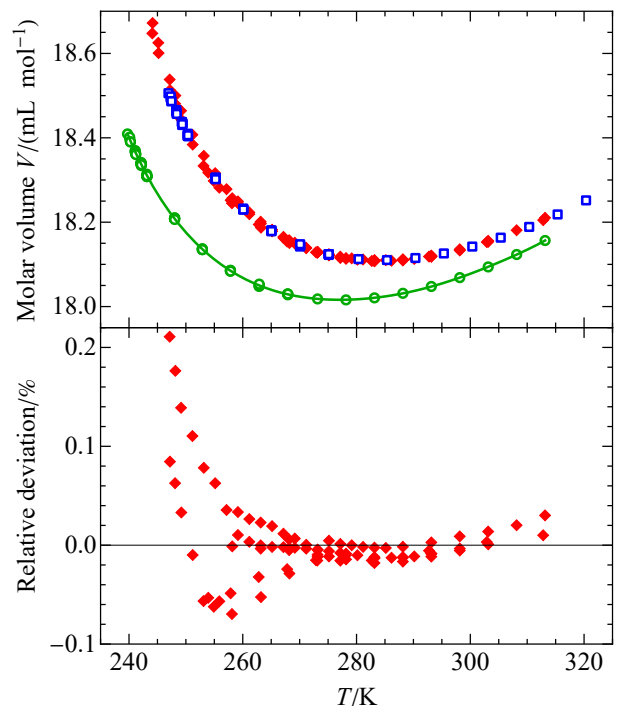


FIG. 2. Molar volume of water. Top panel: data for H₂O (empty green circles) with their fit (green curve), D₂O (filled red diamonds), and results of Eq. 1 applied to H₂O data (empty blue squares). Bottom panel: relative deviation of D₂O data from values calculated using Eq. 1 combined with the fit to H₂O data. Here $\Delta T = 7.2$ K and $\lambda = M_r/1.1059$.

simple relation:

$$X_D(T) = \lambda X_H(T - \Delta T) \quad (1)$$

where X_D and X_H are the values of a property for D₂O and H₂O, respectively, λ is an amplitude factor, and ΔT is a thermal offset.

They first applied this concept to density¹⁴, and obtained excellent results at ambient pressure from 243 to 303 K, with $\Delta T = 7.2$ K, and $\lambda = 1.1059$. In this case, ΔT is obviously the difference between the temperatures of density maximum for the two isotopes. The factor λ is slightly less than the ratio of their molecular weights, $M_r = 20.02292/18.010565 = 1.11173$, which is attributed to slightly different hydrogen-bond distances and atomic root-mean-square displacements. In Fig. 2, we illustrate the results on molar volumes rather than density to more directly show the isotopic difference.

In Ref. 14, they briefly mentioned viscosity, which they investigated in details in a subsequent paper¹⁵. They could reproduce experimental data at ambient pressure to better than 1% below 323 K, using this time $\Delta T = 6.498$ K and $\lambda = \sqrt{M_r}$. This latter value is consistent with the prediction of the gas kinetic Chapman-Enskog theory for hard spheres⁶¹. As shown in Fig. 3, the deviation in fact exceeds 3% at low temperatures. This comes from the fact that, in that range, we used

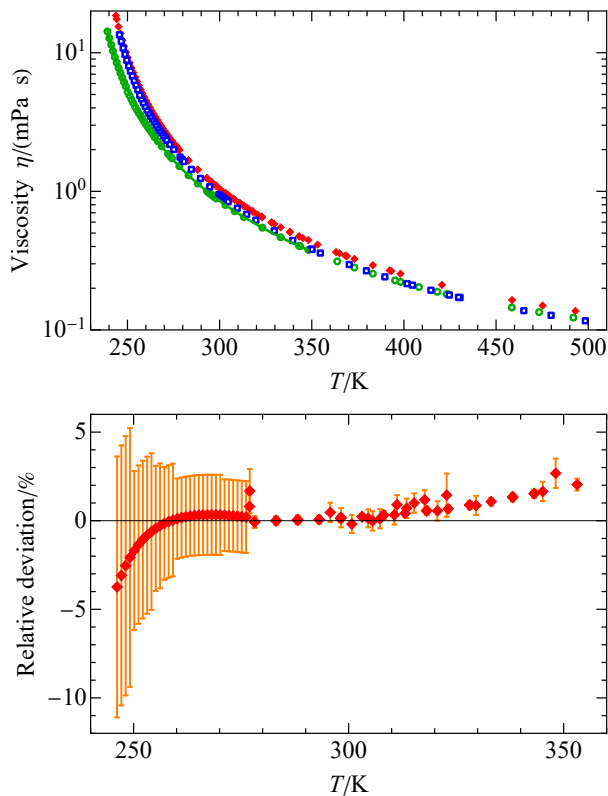


FIG. 3. Shear viscosity of water. Top panel: data for H_2O (empty green circles) with their fit (green curve), for D_2O (filled red diamonds), and results of Eq. 1 applied to H_2O data (empty blue squares). Bottom panel: relative deviation of D_2O data from values calculated using Eq. 1 combined with the fit to H_2O data. Here $\Delta T = 6.498 \text{ K}$ and $\lambda = \sqrt{M_r}$. The error bars indicate one standard deviation.

our low temperature data on H_2O and D_2O ¹¹, instead of the extrapolated values used in Ref. 15 between 243.15 and 268.15 K. Nevertheless, in view of the experimental uncertainties, the collapse remains satisfactory.

Harris pursued the effort, analyzing viscosity and self-diffusion data for water under pressure⁶². He concluded that the thermal offset hypothesis (Eq. 1) with $\Delta T = 6.498 \text{ K}$ holds within experimental uncertainty below 303 K for viscosity up to 900 MPa with $\lambda = \sqrt{M_r}$, and for self-diffusion up to 400 MPa with $\lambda = 1/\sqrt{M_r}$. The Chapman-Enskog prediction is thus again retrieved.

Limitations. Despite its apparent success, the thermal offset approach suffers from two major limitations.

First, the origin of the temperature offset itself is not fully clear. Robinson and co-workers provide a justification based on a mixture model for water, in which the properties of water are obtained by a simple weighted average of two components^{13,14}. The fractions f and $1 - f$ of the two components are temperature dependent, but this dependence would simply be shifted in temperature between isotopes, because of “zero-point effects in the temperature-dependent intermolecular potentials, particularly those related to molecular rotational librations.”¹³

The mixture model used in this approach is rather crude, being that of an ideal mixture, whereas it is thought that non-ideality plays an important role^{63,64}. It is not clear neither why the invoked zero-point effects would just cause a simple shift in temperature. Moreover, the required offset temperature ΔT differs between the density data on the one hand, and the dynamic data on the other hand.

Another difficulty lies in the statement that the Chapman-Enskog law is expected to hold in water, after the thermal offset has been removed. The viscosity ratio is indeed $\sqrt{M_r}$ for isotopes of dilute monatomic gases, but the transposition to dense molecular liquids is not straightforward. Coupling between translation and rotation, possibly temperature dependent, renders the picture rather complex.

For a series of standard solvents near room temperature, Holz *et al.*⁶⁵ found η_r and D_r to be close to each other, and close to $\sqrt{I_r}$ (where $I_r = I_2/I_1$ is the ratio of moments of inertia for the isotopes), rather than to $\sqrt{M_r}$. Holz *et al.* attributed this effect to a strong translation-rotation coupling. This was criticized by Buchhauser *et al.*⁶⁶, who noted that up to three different principal moment of inertia may be defined for a molecule, and pointed out several cases (including water) where D_r varies noticeably with temperature, whereas I_r is constant. Figure 1 shows that, for water, η_r and D_r are always far above $\sqrt{M_r}$, and below 260 K, they both exceed the highest $\sqrt{I_r}$. Figure 1 also shows that, while at temperatures above melting η_r and D_r track each other, they start departing strongly in the supercooled region.

We think it should not be a prerequisite that the dynamic isotope effects would be temperature-independent and equal to a specific value, such as $\sqrt{M_r}$ or $\sqrt{I_r}$. In fact, Cho *et al.* themselves¹⁵, noting the increasing discrepancy with experimental viscosity data at higher temperature, mentioned that an exact agreement “can be obtained by empirically adjusting” ΔT and λ “to give these parameters a temperature dependence”.

CORRESPONDING STATES ANALYSIS

Working hypothesis. We propose here to improve over the thermal offset concept using a corresponding states analysis. Our goal is to provide a physically based explanation for the connection between various thermodynamic and dynamic properties of water isotopes.

Our working hypothesis is that water anomalies are due to a first order liquid-liquid transition (LLT) in the supercooled region. The liquid-liquid critical point (LLCP) terminating this LLT influences the behavior of liquid water in the supercritical region. Since it was first proposed by simulations with the ST2 potential⁵, this hypothesis has increasingly gained support from simulations and experiments³. The existence of a LLT in simulations has been firmly established by state-of-the-art free energy calculations for the ST2 water model⁶⁷, and evidence for a LLCP has been found with the TIP4P/2005 and TIP4P/ice water models⁶⁸. Transient observation of liquid-liquid coexistence in H_2O has been reported ex-

perimentally⁶⁹.

The corresponding states analysis consists in writing the equation of state of water in reduced temperature-pressure ($T - P$) coordinates $\hat{T} = T/T_c$ and $\hat{P} = P/P_c$:

$$V(T, P) = \frac{RT_c}{P_c} \hat{V}(\hat{T}, \hat{P}), \quad (2)$$

with V the molar volume, R the gas constant, T_c and P_c the temperature and pressure of the LLCP, respectively, and \hat{V} a non-dimensional universal function. Note that Eq. 2 corresponds to the modified corresponding states principle first proposed by Su¹⁷. The quantity RT_c/P_c is used as the volume scale, instead of the critical molar volume V_c . The two choices are equivalent for fluids with equal critical compressibility factors $Z_c = P_c V_c / (RT_c)$. However, in the case of the liquid-vapor critical point, Eq. 2 performs better in giving a universal description of many fluids with various Z_c ¹⁷.

We thus assume that the main isotope effect is to change (T_c, P_c) , but not the function \hat{V} , allowing a mapping of properties of light and heavy water. The mapping should work best at low temperature and in the supercooled liquid region, where the influence of the LLCP is stronger. We will investigate how this hypothesis applies to experimental data in the following.

Molar volume. As in Ref. 14, we first consider the molar volumes at ambient pressure, V_H and V_D for light and heavy water, respectively. Because P_c is estimated to exceed 50 MPa (see Discussion), we assume $\hat{P} \simeq 0$ at ambient pressure. Eq. 2 then predicts the following relation:

$$V_D(T) = \frac{\Theta}{\Pi} V_H \left(\frac{T}{\Theta} \right) \text{ with } \Theta = \frac{T_{c,D}}{T_{c,H}} \text{ and } \Pi = \frac{P_{c,D}}{P_{c,H}}. \quad (3)$$

To obtain Θ and Π , we proceed as follows. We first take molar volumes of light water at $P = 0.1$ MPa from the data listed in Table I. We fit them with a 8-th order polynomial in T , which reproduces the data within their uncertainties. For heavy water, we take molar volumes at $P = 0.1$ MPa from the data listed in Table II. Finally, we make a least-squares fit with Eq. 3, using the 8-th order polynomial for V_H . We progressively include D₂O data points at lower temperatures, until there is no supporting H₂O data available at the corresponding temperature T/Θ , which excludes 4 points below 246 K. This procedure yields $\Theta = 1.031$ and $\Pi = 1.026$.

Figure 4 shows the comparison between experimental and calculated molar volumes for heavy water. The calculation is slightly below the experiment at high temperature, but within the data scatter at low temperature. Indeed, in the supercooled region, as noted in Ref. 2, “there are differences of up to 0.14% between the data sets, and it is not clear which is the best set.” Moreover, the uncertainties are not provided in some of the sources, making it difficult to assess the uncertainties on Θ and Π . We tried repeating the procedure after excluding the data sets which reach the lowest temperatures, Refs. 39 or 40,

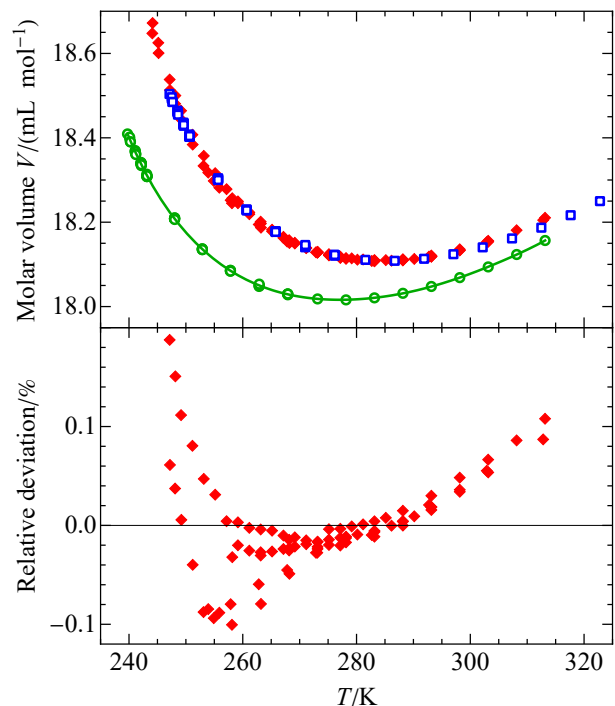


FIG. 4. Molar volume of water. Top panel: data for H₂O (empty green circles) with their fit (green curve), for D₂O (filled red diamonds), and results of Eq. 3 applied to H₂O data (empty blue squares). Bottom panel: relative deviation of D₂O data from values calculated using Eq. 3 combined with the fit to H₂O data. Here $\Theta = 1.031$ and $\Pi = 1.026$.

or both. We obtained for (Θ, Π) the values $(1.029, 1.023)$, $(1.031, 1.026)$, and $(1.027, 1.021)$, respectively.

The corresponding states analysis achieves a similar accuracy as the thermal offset approach¹⁴ (Fig. 2), except at the highest temperatures. Overall, the agreement is satisfactory, as the influence of the LLCP, if it exists, is expected to be stronger at low temperature.

Isothermal compressibility. Isothermal compressibility $\kappa_T = -(1/V)(\partial V/\partial P)_T$ is central to the discussion of the putative LLCP in water, because κ_T should diverge at this LLCP, and show maxima along isobars at pressures below P_c .

Robinson and collaborators considered only compressibility in H₂O⁷⁰ but did not attempt to apply the thermal offset hypothesis. Kim *et al.*⁷¹ observed that κ_T of D₂O at 50 MPa could be superimposed on H₂O data after a 6 K shift. Here we try the corresponding states analysis. Writing κ_H and κ_D for light and heavy water, respectively, and assuming $\hat{P} \simeq 0$, Eq. 2 predicts the following relation:

$$\kappa_D(T) = \frac{1}{\Pi} \kappa_H \left(\frac{T}{\Theta} \right). \quad (4)$$

To test Eq. 4, we use data from Kanno and Angell who measured κ_T for both isotopes in the supercooled region at the same pressures²². Figure 5 shows an excellent agreement at low temperature for 10 MPa. This is

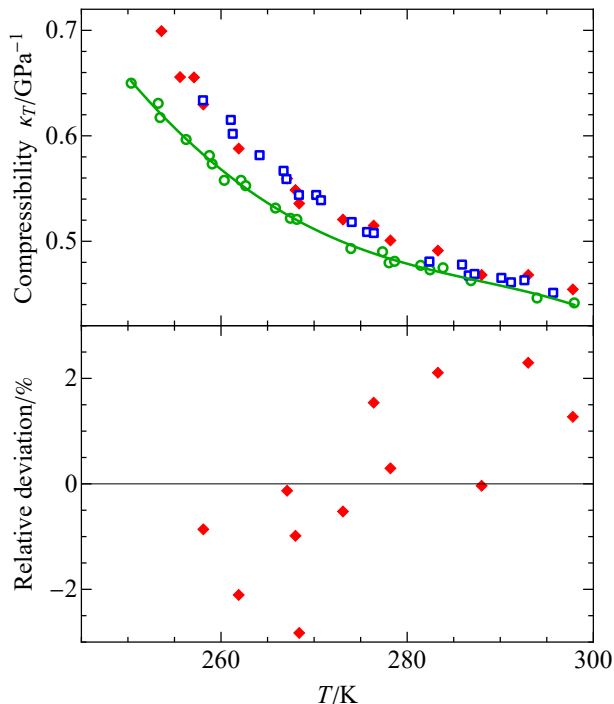


FIG. 5. Isothermal compressibility of water at 10 MPa. Top panel: data for H₂O (empty green circles) with their fit (green curve), for D₂O (filled red diamonds), and results of Eq. 4 applied to H₂O data (empty blue squares). Bottom panel: relative deviation of D₂O data from values calculated using Eq. 4 combined with the fit to H₂O data. Here $\Theta = 1.031$ and $\Pi = 1.026$.

noteworthy as we did not use any further fitting parameters than Θ and Π determined from the molar volumes. A good agreement is also observed at low temperature for other pressures (see the Appendix). As the pressure increases, the experimental D₂O data tend to be higher than the prediction with Eq. 4. We note however that, in principle, the comparison should be made at the same value of P/P_c . For instance, when using the 100 MPa data for light water, heavy water data at 102.6 MPa should be used instead of 100 MPa. From Ref. 22, we estimate this would decrease the experimental values by $\simeq 1.5\%$, thus improving the agreement with the prediction.

Isobaric heat capacity. We now consider the isobaric heat capacity C_P , and test the following relation:

$$C_{P,D}(T) = C_{P,H} \left(\frac{T}{\Theta} \right). \quad (5)$$

The only measurement on supercooled D₂O was performed at ambient pressure by Angell *et al.*²³. There are several measurements for supercooled H₂O, but they show some discrepancies; we used Ref. 23 for consistency because both isotopes were measured in the same setup, and also because this experiment achieved the largest supercooling. Figure 6 shows that the increase in C_P upon cooling starts at higher temperature for D₂O, but

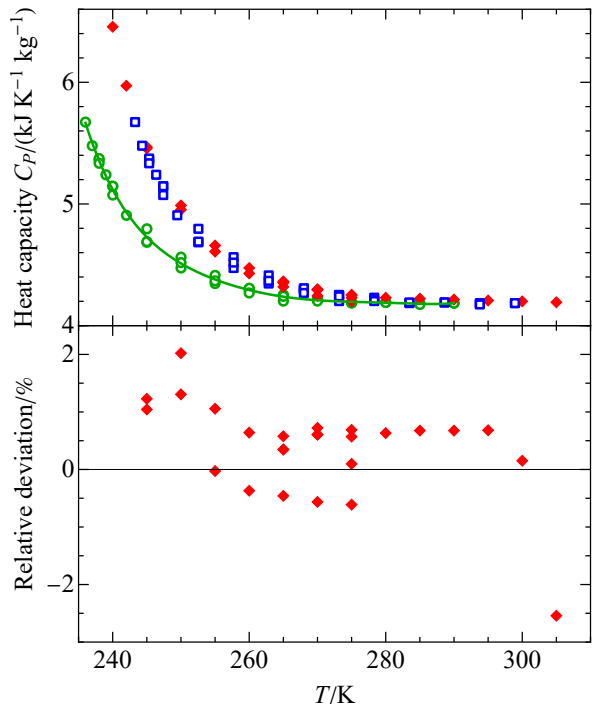


FIG. 6. Isobaric heat capacity of water. Top panel: data for H₂O (empty green circles) with their fit (green curve), for D₂O (filled red diamonds), and results of Eq. 5 applied to H₂O data (empty blue squares). Bottom panel: relative deviation of D₂O data from values calculated using Eq. 5 combined with the fit to H₂O data. Here $\Theta = 1.031$.

the two data sets are superimposed after multiplying the temperatures of the H₂O data by Θ . This is actually surprising, because Fig. 6 involves heat capacities per unit mass, rather than the molar heat capacities, which would differ by 11%. We note that the principle of corresponding states does not strictly apply to heat capacity. Indeed, in the case of the liquid-vapor transition, Guggenheim pointed out in his seminal work¹⁶ that the molar C_P scales as expected for monatomic fluids, but only approximately for diatomic molecules, the difference from monatomic fluids exceeding the theoretical free rotor contribution. Guggenheim attributed this to “a small restriction of the rotation increasing with decreasing temperature”. Water molecules do not rotate freely, and possess vibrational degrees of freedom; it seems that the various contributions to heat capacity per unit mass become identical for the two isotopes after the temperature is rescaled. Understanding the isotopic effect on C_P will require further investigation.

Dynamic properties. We now turn to dynamic properties. In contrast to the thermal offset hypothesis, we do not attempt to achieve a perfect rescaling. Indeed, as discussed above, there is no compelling reason that the isotopic ratio for dynamic quantities in molecular liquids should exactly scale as $\sqrt{M_r}$. Therefore, for a dynamic quantity X , we rather plot a *rescaled* isotopic ratio after

rescaling the temperature:

$$\tilde{X}_r = \frac{X_D(T)}{X_H(T/\Theta)}. \quad (6)$$

Here the subscripts H and D stand for light and heavy water, respectively. Figure 7 shows the results for $X = \eta$, $1/D$, and τ_θ , respectively. The H₂O data (Table I) were fitted with Speedy-Angell laws:

$$X = X_0 \left(\frac{T}{T_s} - 1 \right)^{-\gamma}, \quad (7)$$

for use in Eq. 6.

The raw isotopic ratios η_r , D_r , and $\tau_{\theta,r}$ reach high values at low temperature: 2.38, 1.66, and 3.26, respectively (see Fig. 1). After rescaling the temperature, we see that all ratios lie close to $\sqrt{M_r}$, but systematic deviations are observed. Still, it is interesting to see that the amplitude of the dynamic isotope effect is much reduced after this temperature rescaling, making it similar to a number of other molecular liquids.

Violation of the Stokes-Einstein relation. We believe another approach is required to apply the corresponding states analysis to dynamic quantities. We propose to use the Stokes-Einstein relation (SER). For a Brownian sphere of radius R in a liquid with shear viscosity η , the diffusion coefficient D obeys the SER: $D = k_B T / (C\pi\eta R)$, where k_B is the Boltzmann constant, and C a coefficient ranging from 6 to 4 for no-slip to full-slip boundary conditions, respectively^{72,73}. It follows that the Stokes-Einstein ratio (SE ratio), $D\eta/T$, is temperature-independent. Usually, for a molecule of a liquid, the constancy of $D\eta/T$ (using now the self-diffusion coefficient D), holds at high temperature but fails when the temperature decreases below around $1.3T_g$, where T_g is the glass transition temperature⁷⁴. The violation in water already starts at ambient conditions, which corresponds to above $2T_g$ ¹⁰.

Our previous work on shear viscosity η of supercooled light water¹⁰, combined with literature data on the self-diffusion coefficient³⁴ and the rotational correlation time³⁶, revealed that the viscosity of water remains coupled with rotation in a fashion similar to usual glass-formers, while it strongly decouples from translation. In particular, the SE ratio remains constant above room temperature but strongly increases upon cooling. Our recently obtained viscosity values in supercooled heavy water¹¹ confirmed a similar trend for the SER (see Fig. 8, top panel).

When the SER holds, we can compute an apparent hydrodynamic radius R_h , defined by inverting the SER: $R_h = k_B T / (C\pi D_s \eta)$. As shown in Ref. 11, above 280 K, R_h is nearly the same for the two isotopes: 0.16 or 0.11 nm with $C = 4$ or 6, respectively. This common R_h value is also close to the size of a water molecule, which is virtually the same for H₂O and D₂O, as their molar volumes differ only marginally. The SER is thus fulfilled above 300 K¹¹. A close look at Fig. 8 reveals that the

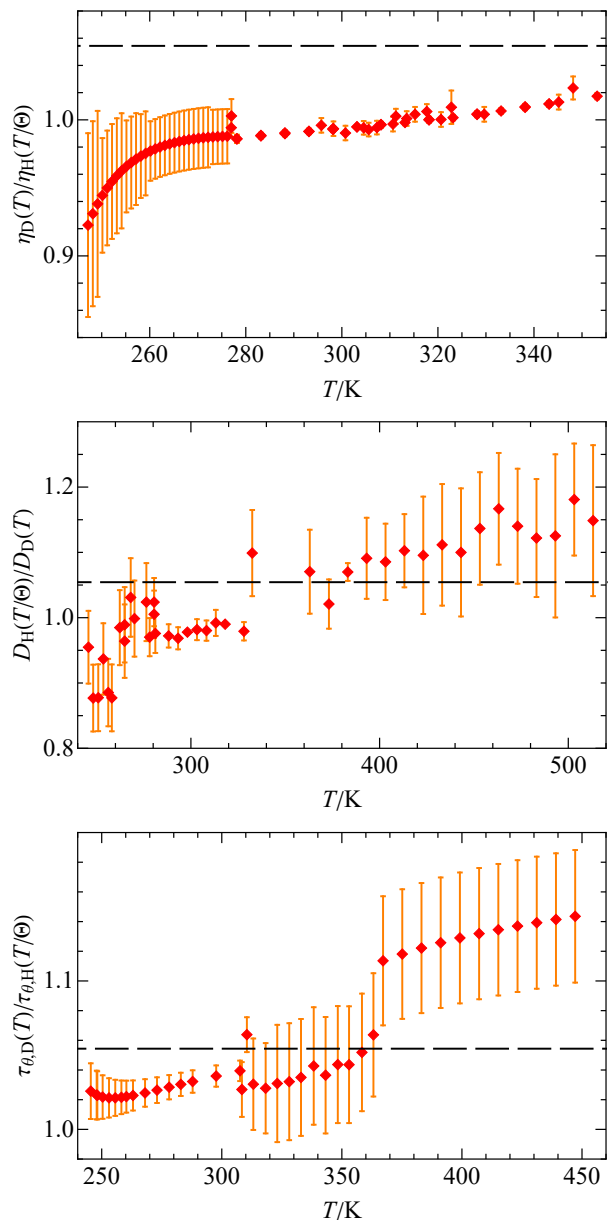


FIG. 7. Rescaled isotopic ratio \tilde{X}_r for $X = \eta$ (top), $1/D$ (middle), and τ_θ (bottom), using Eq. 6 with $\Theta = 1.031$. The error bars indicate one standard deviation. The horizontal dashed lines show $\sqrt{M_r}$.

SER ratio above 370 K is systematically slightly higher for H₂O than for D₂O. However, these H₂O values are based on D from Ref. 32. Ref. 55 provides another set of D values in this temperature range, which are consistent within uncertainty with Ref. 32, but around 10% lower. Using the lower values would reconcile the SER ratios for both isotopes at high temperature.

In contrast, at low temperature, SER is violated: the SE ratio increases sharply (see Fig. 8), and the calculated R_h values become unphysically small, dropping by 40% from 298 to 244 K, and cannot be interpreted as a molecular size any more. The SER violation is usually at-

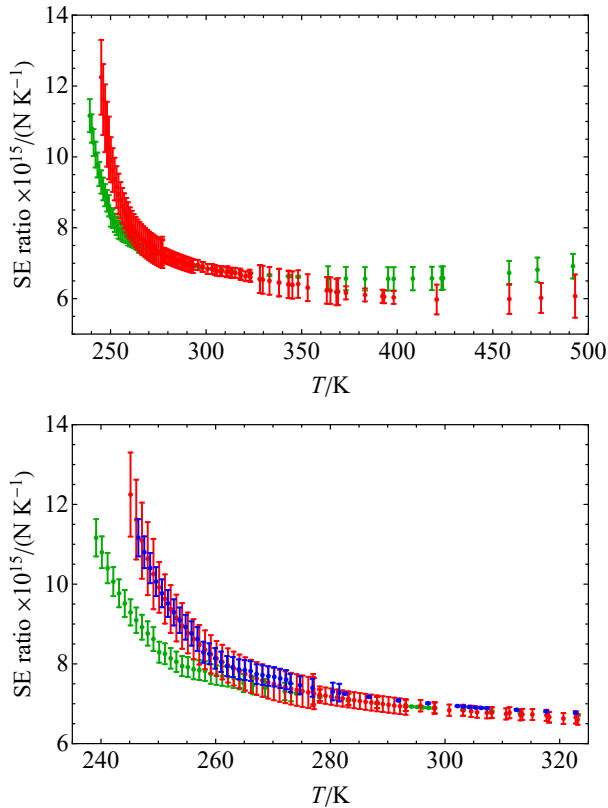


FIG. 8. Stokes-Einstein ratio $D\eta/T$ for light water (green) and heavy water (red) (top panel). The bottom panel shows a close-up at low temperature, adding light water data after multiplying their temperatures by $\Theta = 1.031$ (blue). Error bars indicate one standard deviation.

tributed to decoupling between viscosity and translation, due to collective effects¹⁰. The distribution of relaxation times in the system, rather narrow at high temperature, broadens at low temperature and η and D decouple because they are related to different moments of this distribution⁷⁵. The fact that the two data sets in Fig. 8 run parallel to each other suggests that H_2O and D_2O experience similar collective effects, albeit starting at different temperatures. We may thus attempt the same corresponding states analysis, plotting the data for SE ratio in light water after multiplying their temperatures by Θ . The result falls on top of the SE ratio in heavy water, see Fig. 8 (bottom panel). We argue that the direct comparison of the SE ratio $D\eta/T$ avoids the complications encountered with the prefactor introduced for the dynamic properties.

It would be interesting to repeat this analysis at higher pressure. We recently showed that the SE ratios for H_2O along various isobars are qualitatively similar. At room temperature, the apparent R_h values are nearly equal at all pressures, but the SER violation starts at lower temperature under pressure⁷⁶. Unfortunately, along isobars at pressures above ambient, viscosity data for D_2O extends at most 3 K below the melting point of each iso-

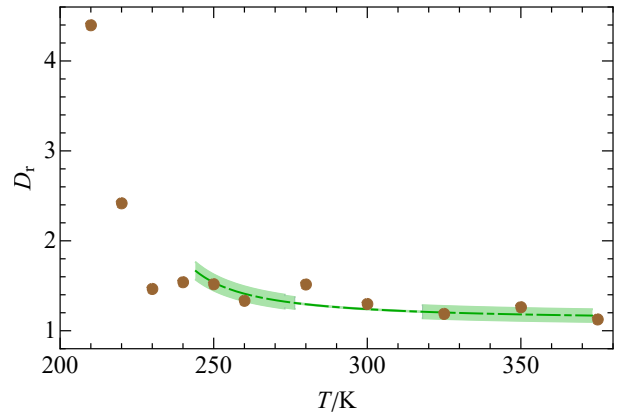


FIG. 9. Isotope effect as a function of temperature for self-diffusion D_r from the experiments (dash-dotted green curve) and path-integral molecular dynamics simulations⁷⁷ (filled brown circles). The colored area denote $1 - \sigma$ uncertainty.

bar⁴⁹. Only the high temperature, rather flat part of the SE curves can thus be plotted for pressurized D_2O ; within experimental uncertainty, they are compatible with both the raw and temperature-rescaled SE curves for H_2O . This calls for further viscosity measurements in supercooled D_2O under pressure.

DISCUSSION

We have thus shown that molar volumes of light and heavy water can be superimposed in a corresponding states analysis, by choosing appropriate values of the parameters $\Theta = 1.031$ and $\Pi = 1.026$ in Eq. 3. Moreover, using fixed values for these parameters, a remarkable collapse is also achieved for isothermal compressibility and for the Stokes-Einstein ratio.

If a LLT does exist in supercooled water, the collapse of isothermal compressibility is expected as a consequence of the critical behavior dictating the divergence of κ_T at the LLCPC, and its reaching maxima along the Widom line emanating from the LLCPC³. Actually, κ_T maxima along isobars have been reported in H_2O at negative pressure⁷⁸, and in both H_2O and D_2O at near-zero pressure⁷⁹. We can further test Eq. 4 on this latter study, computing the ratios of temperatures and amplitudes for the respective maxima in D_2O ($233.0(10) \text{ K}$, $97.5(5) \times 10^{-5} \text{ MPa}^{-1}$) and H_2O ($229.2(10) \text{ K}$, $104.5(10) \times 10^{-5} \text{ MPa}^{-1}$). The corresponding parameters would be $\Theta = 1.017 \pm 0.006$ and $\Pi = 1.07 \pm 0.01$. This values are close to, but significantly different from, our values determined from the molar volumes. We note however that the exact location, and even existence, of the κ_T maxima at $P = 0$ is a matter of debate^{80,81}.

A further comparison of Θ and Π can be made using previous estimates of the LLCPC coordinates for H_2O and D_2O . Interpreting his classic experiments on decompression- and compression-induced melting of high-pressure ices, Mishima proposed for the LLCPC location ($T_c \simeq 220 \text{ K}$, $P_c \simeq 100 \text{ MPa}$)⁷ and ($T_c =$

230(5) K, $P_c \simeq 50(20)$ MPa⁹ for H₂O and D₂O, respectively. Later, analyzing volumes of supercooled H₂O, Mishima revised the LLC location to ($T_c \simeq 223$ K, $P_c \simeq 50$ MPa)⁸². Taking Mishima's most recent estimates would give $\Theta \simeq 230/223 = 1.03$ and $\Pi \simeq 1$, in line with our values. In recent path-integral molecular dynamics simulations, Giovambattista and collaborators included from first principles nuclear quantum effects in the study of the phase diagram of water⁸³. Their approach quantitatively captures the isotope effects on molar volumes and self-diffusion (see Fig. 9). They reported LLT in both isotopes, with ($T_c = 159(6)$ K, $P_c = 167(9)$ MPa) and ($T_c = 177(3)$ K, $P_c = 176(2)$ MPa) for H₂O and D₂O, respectively. This yields $\Theta = 1.11 \pm 0.05$ and $\Pi = 1.05 \pm 0.06$, compatible with our values. We also note that both studies suggest a rather large value for P_c , so that $P = 0.1$ MPa can be treated as $\bar{P} \simeq 0$.

We now turn to the origin of the collapse for the SE ratio. The violation of the SER in H₂O has been related to the putative liquid-liquid transition in supercooled water by molecular dynamics simulations⁸⁴, phenomenologic two-state modelling⁸⁵, or both⁸⁶. A recent molecular dynamics study⁸⁷ attributes the violation of SER upon cooling to the increasing role of molecular jumps in translational diffusion. When the jumps are removed, the residual diffusion due to cage trajectories of the molecules fulfills the SER. To explain the difference seen experimentally between isotopes, we propose that the share of jump trajectories in diffusion, due to structural changes in water, varies similarly for both isotopes, once the relative distance to the LLC and the Widom line have been taken into account by the appropriate $T - P$ rescaling.

Structure factors of D₂O measured in the range 240 – 275 K⁷¹ were observed to match the structure factors of H₂O measured $\simeq 5$ K below. The same match can be obtained by rescaling the temperatures by a factor $\simeq 1.02$, close to $\Theta = 1.031$. This gives credence to a structural explanation of the SE ratio collapse.

As just mentioned, a temperature shift closely resembles a temperature rescaling when a limited temperature range is considered. This can be easily seen, writing for a temperature $T_1 \simeq 260$ K the rescaled temperature $T_2 = \Theta T_1 = T_1 + (\Theta - 1)T_1 \simeq T_1 + (\Theta - 1)260$ K = $T_1 + 8$ K. This shows that the comparable success of the two approaches, thermal offset and corresponding states analysis, is no coincidence. We argue that the latter approach is more physically grounded (being connected to the LLC), gives consistent results for a single value of the parameter Θ , and in addition gives an explanation for the amplitude rescaling involving the effect of pressure through Π . Nevertheless, Robinson's intuition is confirmed, and the role of zero-point and nuclear quantum effects is to move the LLC location, as seen in PIMD simulations.

To conclude, the series of results presented here is thus consistent with the putative LLT in supercooled water, and our understanding of its manifestations. It does not

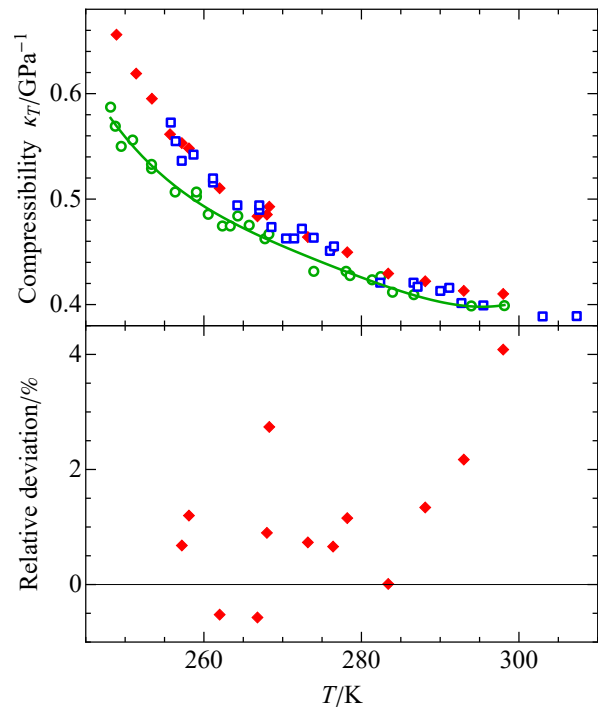


FIG. 10. Isothermal compressibility of water at 50 MPa. Same legend as Fig. 5.

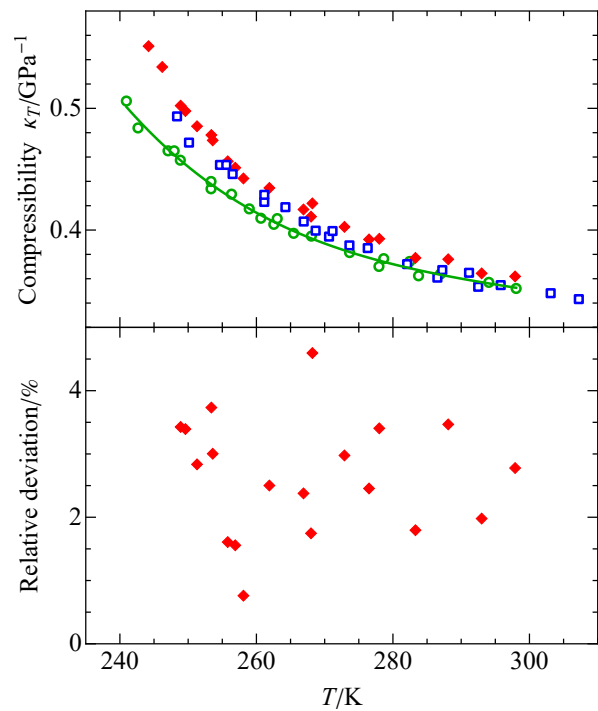


FIG. 11. Isothermal compressibility of water at 100 MPa. Same legend as Fig. 5.

however prove its existence and calls for further work.

ACKNOWLEDGMENTS

We thank Nicolas Giovambattista for providing the simulation data for D_r , Gregory Kimmel for suggesting us to investigate the “corresponding states” approach, and Mikhail A. Anisimov for helpful discussions. We acknowledge support from Agence Nationale de la Recherche, grant number ANR-19-CE30-0035-01.

APPENDIX: Isothermal compressibility under pressure

Figures 10 and 11 show the results of the corresponding states analysis applied to isothermal compressibility data under pressure²².

- ¹M. Francl, “The weight of water,” *Nat. Chem.* **11**, 284–285 (2019).
- ²V. Holtin, C. E. Bertrand, M. A. Anisimov, and J. V. Sengers, “Thermodynamics of supercooled water,” *J. Chem. Phys.* **136**, 094507 (2012).
- ³P. Gallo, K. Amann-Winkel, C. A. Angell, M. A. Anisimov, F. Caupin, C. Chakravarty, E. Lascaris, T. Loerting, A. Z. Panagiotopoulos, J. Russo, J. A. Sellberg, H. E. Stanley, H. Tanaka, C. Vega, L. Xu, and L. G. M. Pettersson, “Water: A tale of two liquids,” *Chem. Rev.* **116**, 7463–7500 (2016).
- ⁴S. Herrig, M. Thol, A. H. Harvey, and E. W. Lemmon, “A reference equation of state for heavy water,” *J. Phys. Chem. Ref. Data* **47**, 043102 (2018).
- ⁵P. H. Poole, F. Sciortino, U. Essmann, and H. E. Stanley, “Phase behaviour of metastable water,” *Nature* **360**, 324–328 (1992).
- ⁶O. Mishima, L. D. Calvert, and E. Whalley, “An apparently first-order transition between two amorphous phases of ice induced by pressure,” *Nature* **314**, 76–78 (1985).
- ⁷O. Mishima and H. E. Stanley, “Decompression-induced melting of ice IV and the liquid–liquid transition in water,” *Nature* **392**, 164–168 (1998).
- ⁸D. Klug, O. Mishima, and E. Whalley, “Raman spectrum of high-density amorphous ice,” *Physica B+C* **139–140**, 475–478 (1986).
- ⁹O. Mishima, “Liquid–liquid critical point in heavy water,” *Phys. Rev. Lett.* **85**, 334–336 (2000).
- ¹⁰A. Dehaoui, B. Isenmann, and F. Caupin, “Viscosity of deeply supercooled water and its coupling to molecular diffusion,” *Proc. Natl. Acad. Sci.* **112**, 12020–12025 (2015).
- ¹¹P. Ragueneau, F. Caupin, and B. Isenmann, “Shear viscosity and Stokes-Einstein violation in supercooled light and heavy water,” *Phys. Rev. E* **106**, 014616 (2022).
- ¹²N. Rudenko and V. Konareva, “Viscosity of liquid hydrogen and deuterium,” *Russ. J. Phys. Chem.* **37**, 1493–1494 (1963).
- ¹³M. Vedamuthu, S. Singh, and G. W. Robinson, “Properties of liquid water: Origin of the density anomalies,” *J. Phys. Chem.* **98**, 2222–2230 (1994).
- ¹⁴M. Vedamuthu, S. Singh, and G. W. Robinson, “Simple relationship between the properties of isotopic water,” *J. Phys. Chem.* **100**, 3825–3827 (1996).
- ¹⁵C. H. Cho, J. Urquidi, S. Singh, and G. W. Robinson, “Thermal offset viscosities of liquid H₂O, D₂O, and T₂O,” *J. Phys. Chem. B* **103**, 1991–1994 (1999).
- ¹⁶E. A. Guggenheim, “The Principle of Corresponding States,” *J. Chem. Phys.* **13**, 253–261 (1945).
- ¹⁷G.-J. Su, “Modified Law of Corresponding States for Real Gases,” *Ind. Eng. Chem.* **38**, 803–806 (1946).
- ¹⁸A. Kostrowicka Wyczalkowska, K. S. Abdulkadirova, M. A. Anisimov, and J. V. Sengers, “Thermodynamic properties of H₂O and D₂O in the critical region,” *J. Chem. Phys.* **113**, 4985–5002 (2000).
- ¹⁹K. S. Abdulkadirova, A. Kostrowicka Wyczalkowska, M. A. Anisimov, and J. V. Sengers, “Thermodynamic properties of mixtures of H₂O and D₂O in the critical region,” *J. Chem. Phys.* **116**, 4597–4610 (2002).
- ²⁰D. E. Hare and C. M. Sorensen, “The density of supercooled water. ii. Bulk samples cooled to the homogeneous nucleation limit,” *J. Chem. Phys.* **87**, 4840–4845 (1987).
- ²¹The International Association for the Properties of Water and Steam, “Revised release on the IAPWS formulation 1995 for the thermodynamic properties of ordinary water substance for general and scientific use,” Tech. Rep. IAPWS R6-95(2018) (The International Association for the Properties of Water and Steam, 2018).
- ²²H. Kanno and C. A. Angell, “Water: Anomalous compressibilities to 1.9 kbar and correlation with supercooling limits,” *J. Chem. Phys.* **70**, 4008–4016 (1979).
- ²³C. A. Angell, W. J. Sichina, and M. Oguni, “Heat capacity of water at extremes of supercooling and superheating,” *J. Phys. Chem.* **86**, 998–1002 (1982).
- ²⁴J. Hallett, “The temperature dependence of the viscosity of supercooled water,” *Proc. Phys. Soc.* **82**, 1046–1050 (1963).
- ²⁵G. Korosi and E. S. Kovats, “Density and surface tension of 83 organic liquids,” *J. Chem. Eng. Data* **26**, 323–332 (1981).
- ²⁶L. D. Eicher and B. J. Zwolinski, “High-precision viscosity of supercooled water and analysis of the extended range temperature coefficient,” *J. Phys. Chem.* **75**, 2016–2024 (1971).
- ²⁷J. Kestin and I. R. Shankland, “The free disk as an absolute viscometer and the viscosity of water in the range 25–150 °C,” *J. Non-Equilib. Thermodyn.* **6**, 241–256 (1981).
- ²⁸A. F. Collings and N. Bajenov, “A high precision capillary viscometer and further relative results for the viscosity of water,” *Metrologia* **19**, 61–66 (1983).
- ²⁹J. Kestin, N. Imaishi, S. H. Nott, J. C. Nieuwoudt, and J. V. Sengers, “Viscosity of light and heavy water and their mixtures,” *Physica A* **134**, 38–58 (1985).
- ³⁰D. Berstad, B. Knapstad, M. Lamvik, P. Skjølsvik, K. Tørklep, and H. Øye, “Accurate measurements of the viscosity of water in the temperature range 19.5–25.5 °C,” *Physica A* **151**, 246–280 (1988).
- ³¹R. Mills, “Self-diffusion in normal and heavy water in the range 1–45°,” *J. Phys. Chem.* **77**, 685–688 (1973).
- ³²K. Krynicki, C. D. Green, and D. W. Sawyer, “Pressure and temperature dependence of self-diffusion in water,” *Faraday Discuss. Chem. Soc.* **66**, 199–208 (1978).
- ³³A. J. Eastale, W. E. Price, and L. A. Woolf, “Diaphragm cell for high-temperature diffusion measurements. tracer diffusion coefficients for water to 363 K,” *J. Chem. Soc., Faraday Trans. 1* **85**, 1091–1097 (1989).
- ³⁴W. S. Price, H. Ide, and Y. Arata, “Self-diffusion of supercooled water to 238K using PGSE NMR diffusion measurements,” *J. Phys. Chem. A* **103**, 448–450 (1999).
- ³⁵J. C. Hindman, “Relaxation processes in water: viscosity, self-diffusion, and spin-lattice relaxation. A kinetic model,” *J. Chem. Phys.* **60**, 4488–4496 (1974).
- ³⁶J. Qvist, C. Mattea, E. P. Sunde, and B. Halle, “Rotational dynamics in supercooled water from nuclear spin relaxation and molecular simulations,” *J. Chem. Phys.* **136**, 204505 (2012).
- ³⁷A. Blahut, J. Hykl, P. Peukert, V. Vinš, and J. Hrubý, “Relative density and isobaric expansivity of cold and supercooled heavy water from 254 to 298 K and up to 100 MPa,” *J. Chem. Phys.* **151**, 034505 (2019).
- ³⁸G. S. Kell, “Precise representation of volume properties of water at one atmosphere,” *J. Chem. Eng. Data* **12**, 66–69 (1967).
- ³⁹B. V. Zheleznyi, “The density of supercooled water,” *Russ. J. Phys. Chem.* **43**, 1311 (1969).
- ⁴⁰D. H. Rasmussen and A. P. MacKenzie, “Clustering in supercooled water,” *J. Chem. Phys.* **59**, 5003–5013 (1973).
- ⁴¹R. T. Emmet and F. J. Millero, “Specific volume of deuterium oxide from 2° to 40°C and 0 to 1000 bars applied pressure,” *J. Chem. Eng. Data* **20**, 351–356 (1975).
- ⁴²H. Kanno and C. A. Angell, “Volumetric and derived thermal characteristics of liquid D₂O at low temperatures and high pressures,” *J. Chem. Phys.* **73**, 1940–1947 (1980).
- ⁴³D. E. Hare and C. M. Sorensen, “Densities of supercooled H₂O

- and D₂O in 25 μ glass capillaries,” *J. Chem. Phys.* **84**, 5085–5089 (1986).
- ⁴⁴R. C. Hardy and R. L. Cottingham, “Viscosity of deuterium oxide and water in the range 5° to 125° C,” *J. Res. Natl. Bur. Stan.* **42**, 573 (1949).
- ⁴⁵A. Selecki, B. Tyminski, and A. G. Chmielewski, “Viscosity of solutions of some electrolytes in heavy water,” *J. Chem. Eng. Data* **15**, 127–130 (1970).
- ⁴⁶F. J. Millero, Roger. Dexter, and Edward. Hoff, “Density and viscosity of deuterium oxide solutions from 5-70°C,” *J. Chem. Eng. Data* **16**, 85–87 (1971).
- ⁴⁷F. Gonçalves, “The viscosity of H₂O + D₂O mixtures in the range 20 - 60°C,” in *Proc. 9th Int. Conf. Properties of Steam, Munich 1979* (Pergamon, Oxford, 1980) J. Straub and K. Scheffler ed., pp. 354–361.
- ⁴⁸N. Agayev, “Experimental investigation of the viscosity of ordinary and heavy water and steam in the temperature range from -10 to 375°C and at pressures from 0.1 to 200 MPa,” in *Proc. 9th Int. Conf. Properties of Steam, Munich 1979* (Pergamon, Oxford, 1980) J. Straub and K. Scheffler ed., pp. 148–154.
- ⁴⁹N. Agayev, “Heavy-water viscosity under high pressures near freezing line,” in *Proc. 11th Int. Conf. Properties of Water and Steam 1989, Prague* (Hemisphere Publishing, 1990) M. Píchal and O. Šifner ed., pp. 148–154.
- ⁵⁰L. A. Woolf, “Tracer diffusion of tritiated heavy water (DTO) in heavy water (D₂O) under pressure,” *J. Chem. Soc., Faraday Trans. 1* **72**, 1267–1273 (1976).
- ⁵¹H. Weingärtner, “Diffusion in liquid mixtures of light and heavy water,” *Ber. Bunsenges. Phys. Chem.* **88**, 47–50 (1984).
- ⁵²F. X. Prielmeier, E. W. Lang, R. J. Speedy, and H.-D. Lüdemann, “The pressure dependence of self diffusion in supercooled light and heavy water,” *Ber. Bunsenges. Phys. Chem.* **92**, 1111–1117 (1988).
- ⁵³W. S. Price, H. Ide, Y. Arata, and O. Söderman, “Temperature dependence of the self-diffusion of supercooled heavy water to 244 K,” *J. Phys. Chem. B* **104**, 5874–5876 (2000).
- ⁵⁴E. H. Hardy, A. Zygari, M. D. Zeidler, M. Holz, and F. D. Sacher, “Isotope effect on the translational and rotational motion in liquid water and ammonia,” *J. Chem. Phys.* **114**, 3174–3181 (2001).
- ⁵⁵K. Yoshida, N. Matubayasi, and M. Nakahara, “Self-diffusion coefficients for water and organic solvents at high temperatures along the coexistence curve,” *J. Chem. Phys.* **129**, 214501 (2008).
- ⁵⁶J. C. Hindman, A. J. Zielen, A. Svirnickas, and M. Wood, “Relaxation processes in water. the spin-lattice relaxation of the deuteron in D₂O and oxygen-17 in H₂¹⁷O,” *J. Chem. Phys.* **54**, 621–634 (1971).
- ⁵⁷J. Jonas, T. DeFries, and D. J. Wilbur, “Molecular motions in compressed liquid water,” *J. Chem. Phys.* **65**, 582–588 (1976).
- ⁵⁸E. Lang and H.-D. Lüdemann, “Pressure and temperature dependence of the longitudinal deuterium relaxation times in supercooled heavy water to 300 MPa and 188 K,” *Ber. Bunsenges. Phys. Chem.* **84**, 462–470 (1980).
- ⁵⁹N. Matubayasi, N. Nakao, and M. Nakahara, “Structural study of supercritical water. III. Rotational dynamics,” *J. Chem. Phys.* **114**, 4107–4115 (2001).
- ⁶⁰J. Ropp, C. Lawrence, T. C. Farrar, and J. L. Skinner, “Rotational motion in liquid water is anisotropic: a nuclear magnetic resonance and molecular dynamics simulation study,” *J. Am. Chem. Soc.* **123**, 8047–8052 (2001).
- ⁶¹S. Chapman and T. G. Cowling, *The Mathematical Theory of Non-uniform Gases: An Account of the Kinetic Theory of Viscosity, Thermal Conduction and Diffusion in Gases* (Cambridge University Press, 1990).
- ⁶²K. R. Harris, “Isotope effects and the thermal offset effect for diffusion and viscosity coefficients of liquid water,” *Phys. Chem. Chem. Phys.* **4**, 5841–5845 (2002).
- ⁶³M. A. Anisimov, M. Duška, F. Caupin, L. E. Amrhein, A. Rosenbaum, and R. J. Sadus, “Thermodynamics of fluid polyamorphism,” *Phys. Rev. X* **8**, 011004 (2018).
- ⁶⁴F. Caupin and M. A. Anisimov, “Thermodynamics of supercooled and stretched water: Unifying two-structure description and liquid-vapor spinodal,” *J. Chem. Phys.* **151**, 034503 (2019).
- ⁶⁵M. Holz, X.-a. Mao, D. Seiferling, and A. Sacco, “Experimental study of dynamic isotope effects in molecular liquids: Detection of translation-rotation coupling,” *J. Chem. Phys.* **104**, 669–679 (1996).
- ⁶⁶J. Buchhauser, T. Groß, N. Karger, and H.-D. Lüdemann, “Self-diffusion in CD₄ and ND₃: with notes on the dynamic isotope effect in liquids,” *J. Chem. Phys.* **110**, 3037–3042 (1999).
- ⁶⁷J. C. Palmer, F. Martelli, Y. Liu, R. Car, A. Z. Panagiotopoulos, and P. G. Debenedetti, “Metastable liquid-liquid transition in a molecular model of water,” *Nature* **510**, 385–388 (2014).
- ⁶⁸P. G. Debenedetti, F. Sciortino, and G. H. Zerze, “Second critical point in two realistic models of water,” *Science* **369**, 289–292 (2020).
- ⁶⁹K. H. Kim, K. Amann-Winkel, N. Giovambattista, A. Späh, F. Perakis, H. Pathak, M. L. Parada, C. Yang, D. Mariedahl, T. Eklund, Thomas. J. Lane, S. You, S. Jeong, M. Weston, J. H. Lee, I. Eom, M. Kim, J. Park, S. H. Chun, P. H. Poole, and A. Nilsson, “Experimental observation of the liquid-liquid transition in bulk supercooled water under pressure,” *Science* **370**, 978–982 (2020).
- ⁷⁰M. Vedamuthu, S. Singh, and G. W. Robinson, “Properties of Liquid Water. 4. The Isothermal Compressibility Minimum near 50 °C,” *J. Phys. Chem.* **99**, 9263–9267 (1995).
- ⁷¹K. H. Kim, H. Pathak, A. Späh, F. Perakis, D. Mariedahl, J. A. Sellberg, T. Katayama, Y. Harada, H. Ogasawara, L. G. M. Pettersson, and A. Nilsson, “Temperature-independent nuclear quantum effects on the structure of water,” *Phys. Rev. Lett.* **119** (2017), 10.1103/PhysRevLett.119.075502.
- ⁷²W. Sutherland, “The measurement of large molecular masses,” in *Rep. Tenth Meet. Australas. Assoc. Adv. Sci.* (Geo. M. Thomson, Dunedin, 1904) pp. 117–121.
- ⁷³W. Sutherland, “A dynamical theory of diffusion for non-electrolytes and the molecular mass of albumin,” *Phil. Mag.* **9**, 781–785 (1905).
- ⁷⁴I. Chang and H. Sillescu, “Heterogeneity at the glass transition: Translational and rotational self-diffusion,” *J. Phys. Chem. B* **101**, 8794–8801 (1997).
- ⁷⁵M. D. Ediger, “Spatially heterogeneous dynamics in supercooled liquids,” *Annu. Rev. Phys. Chem.* **51**, 99–128 (2000).
- ⁷⁶A. Mussa, R. Berthelard, F. Caupin, and B. Isenmann, “Viscosity and Stokes-Einstein relation in deeply supercooled water under pressure,” *J. Chem. Phys.* **159**, 151103 (2023).
- ⁷⁷A. Eltareb, G. E. Lopez, and N. Giovambattista, “Nuclear quantum effects on the thermodynamic, structural, and dynamical properties of water,” *Phys. Chem. Chem. Phys.* **23**, 6914–6928 (2021).
- ⁷⁸V. Holten, C. Qiu, E. Guillermin, M. Wilke, J. Rička, M. Frenz, and F. Caupin, “Compressibility anomalies in stretched water and their interplay with density anomalies,” *J. Phys. Chem. Lett.* **8**, 5519–5522 (2017).
- ⁷⁹K. H. Kim, A. Späh, H. Pathak, F. Perakis, D. Mariedahl, K. Amann-Winkel, J. A. Sellberg, J. H. Lee, S. Kim, J. Park, K. H. Nam, T. Katayama, and A. Nilsson, “Maxima in the thermodynamic response and correlation functions of deeply supercooled water,” *Science* **358**, 1589–1593 (2017).
- ⁸⁰F. Caupin, V. Holten, C. Qiu, E. Guillermin, M. Wilke, M. Frenz, J. Teixeira, and A. K. Soper, “Comment on “Maxima in the thermodynamic response and correlation functions of deeply supercooled water”,” *Science* **360**, eaat1634 (2018).
- ⁸¹K. H. Kim, A. Späh, H. Pathak, F. Perakis, D. Mariedahl, K. Amann-Winkel, J. A. Sellberg, J. H. Lee, S. Kim, J. Park, K. H. Nam, T. Katayama, and A. Nilsson, “Response to comment on “Maxima in the thermodynamic response and correlation functions of deeply supercooled water”,” *Science* **360**, eaat1729 (2018).
- ⁸²O. Mishima, “Volume of supercooled water under pressure and the liquid-liquid critical point,” *J. Chem. Phys.* **133**, 144503 (2010).

- ⁸³A. Eltareb, G. E. Lopez, and N. Giovambattista, “Evidence of a liquid–liquid phase transition in H₂O and D₂O from path-integral molecular dynamics simulations,” *Sci. Rep.* **12**, 6004 (2022).
- ⁸⁴P. Kumar, S. V. Buldyrev, S. R. Becker, P. H. Poole, F. W. Starr, and H. E. Stanley, “Relation between the Widom line and the breakdown of the Stokes–Einstein relation in supercooled water,” *Proc. Natl. Acad. Sci. U.S.A.* **104**, 9575–9579 (2007).
- ⁸⁵L. P. Singh, B. Isenmann, and F. Caupin, “Pressure dependence of viscosity in supercooled water and a unified approach for thermodynamic and dynamic anomalies of water,” *Proc. Natl. Acad. Sci.* **114**, 4312–4317 (2017).
- ⁸⁶P. Montero de Hijes, E. Sanz, L. Joly, C. Valeriani, and F. Caupin, “Viscosity and self-diffusion of supercooled and stretched water from molecular dynamics simulations,” *J. Chem. Phys.* **149**, 094503 (2018).
- ⁸⁷S. Dueby, V. Dubey, and S. Daschakraborty, “Decoupling of translational diffusion from the viscosity of supercooled water: Role of translational jump diffusion,” *J. Phys. Chem. B* **123**, 7178–7189 (2019).